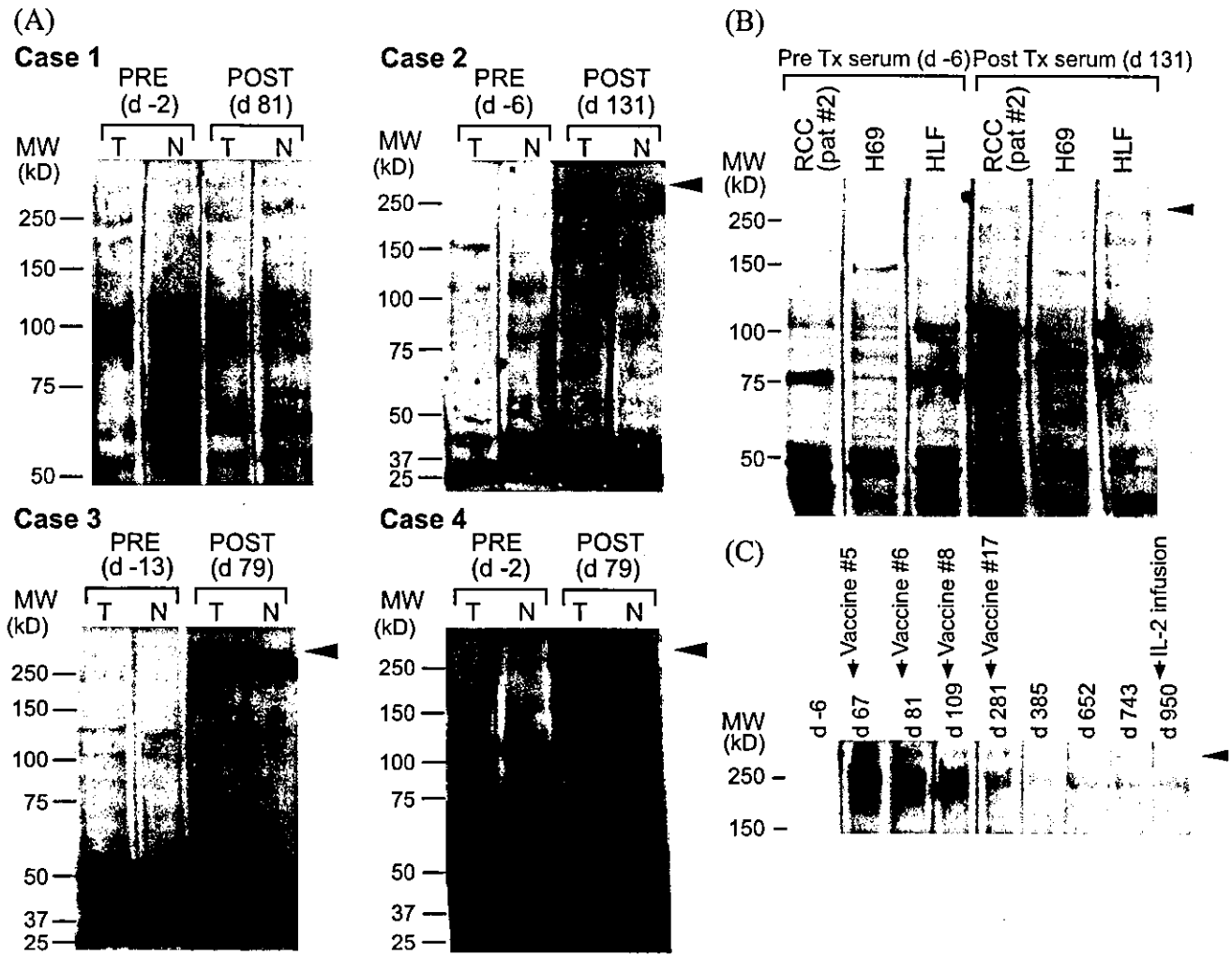

FIG. 6. Appearance of antitumor antibody responses in Cases 1 to 4, who received GVAX. (A) Comparisons of serum reactivity to autologous RCC proteins pre-GTx and post-GTx. Proteins extracted from cultured tumor cells (lane T) or normal kidney cells (lane N) were electrophoresed, transferred onto PVDF membranes, and detected with autologous patient sera (Cases 1 to 4). Sera were harvested before (PRE) and after (POST) the first vaccination (day 0). (B) Comparison of the serum reactivity to autologous RCC, H69 cells, and human lip fibroblasts (HLF). The reactivity to high-molecular-weight proteins was significant in autologous RCC and HLF, while it was weak in H69 cells. Autologous RCC from Case 2 (pat #2) was used. (C) Time course of changes in serum reactivity to high-molecular-weight proteins of approximately 250 kDa in Case 2. Immunoblotting of RCC proteins from Case 2 with autologous sera harvested at several postvaccination days (post-5th, 6th, 8th, and 17th vaccination and before the administration of low-dose IL-2).

investigate pathologically the RCC before and after vaccinations in Case 1 and have demonstrated the induction of tumor site-specific infiltration of predominantly $CD8^+$ T cells. This was associated with tumor apoptosis in postvaccinated biopsy and autopsy tumor specimens, whereas $CD4^+$ T cells predominated and tumor cell apoptosis was negligible in the original RCC (Fig. 3). Notably, these changes were demonstrated in the biopsy specimen that was obtained before IL-2 administration. These observations strongly suggest the induction of tumor-specific immunity by GVAX. Although GVAX could induce both the localization of $CD8^+$ cells within metastatic tumors and significant apoptosis, not all of the tumors showed regression. Thus, GVAX-induced antitumor immunity per se may not be sufficient for clinical efficacy.

We studied various parameters, as it is still unknown which immune factors can be used to predict the therapeutic efficacy of antitumor immune gene therapy. The results of our *in vitro* assessment of cytokine production were compatible to those reported by Soiffer *et al.* [13]. These cytokine profiles indicated the coordinate expression of gene products associated with both Th1 and Th2 cells and suggested that multiple lymphocyte effector mechanisms contribute to the potent antitumor immune response. The cytokines produced by

doi:10.1016/j.ymthe.2004.07.001

these $CD4^+$ T cells activate eosinophils, as well as macrophages that produce both superoxide and nitric oxide. Both of these cell types then collaborate at the site of the tumor challenge to cause its destruction [13]. Our observation suggested that this Th2-dominant immunological response was particularly enhanced, namely, an *in vivo* immune shift from Th1 dominance to Th2 dominance was induced after repeated vaccinations and maintained. Previous studies of GM-CSF immune gene therapy assayed cytotoxicity using PBMC or TIL [13–15]. Kusumoto *et al.* reported that vaccination with irradiated autologous GM-CSF-producing melanoma cells appeared to increase the cytotoxicity against autologous tumor cells in five patients, although repeated vaccination appeared to decrease the CTL activity in two of these cases. They suggested that vaccination of these patients with autologous melanoma cells caused T cell anergy or tolerance [14] without demonstrating the precise underlying immune mechanism involved. In the present study, Case 1, with large lung metastases, which might have contributed to the observed immunological suppression, showed similar results. Although cytotoxicity assayed using PBMC gradually decreased in Case 1, our pathological findings in the metastatic lesion showed the predominant infiltration by CD8 T cells. These findings might support the limited predictability of the *in vivo* antitumor reaction using only traditional immunoassays using PBMC.

Recently, T cell receptor β chain repertoire analysis methods were reported to facilitate the detection of clonal T cell expansion in various biological specimens. As RCC is thought to be a tumor whose growth may be controlled by the immune response, characterization of T lymphocytes found in RCC patients may demonstrate this important issue [16,17]. Using CDR3 length pattern analysis, Puisseux *et al.* demonstrated a selective localization of oligoclonal T cell populations in malignant tissues after comparisons to the T cell repertoire in the tumor and in the autologous peripheral blood lymphocytes or normal adjacent kidney [16]. Importantly, in our clinical studies, the induction of oligoclonal expansion of T cells with the selected TCR in the peripheral blood, skin biopsy specimens from DTH sites, and tumors was demonstrated after vaccination. The reasons for the observed different clonal T cell expansions in the different tissues in our studies may arise from either a polymorphic T cell response to the same antigen or a different immunogenic environment [17]. Hanada *et al.* recently demonstrated the important role of posttranslational protein splicing in the immune recognition of self and foreign peptides using human RCC antigens, and this phenomenon may explain our results [29]. Although we could not prove directly that these oligoclonally expanded T cells responded to RCC antigens, our findings of the generation of MHC-restricted and TCR-mediated cytotoxicity against autologous RCC and the predominant infiltration of CD8 T cells and apoptosis in metastatic lesions [1] supported this possibility.

In addition to the enhanced antitumor cellular immunity, GVAX is thought to induce antitumor humoral immunity. Simons *et al.* measured increased titers of antibodies recognizing prostate tumor antigens in sera from patients vaccinated with GM-CSF-transduced autologous prostate tumor cells. New antibodies recognizing polypeptides of 26, 31, and 150 kDa in extracts from LN CapPCA cells were observed in three of eight patients following the final vaccinations [18]. Soiffer *et al.* reported similar observations, with antibodies recognizing different polypeptides, in melanoma patients [13]. In the present study, Western blot analysis identified RCC-derived polypeptides of 65 and 250 kDa. We are currently screening RCC cDNA expression libraries with our patients' sera using the SEREX method to look for RCC-specific antigens other than RAGE and G250 [30,31]. We have already cloned several candidate cDNAs and are studying their RCC specificities and the possibility of their future application in anti-RCC immunotherapy.

Currently, several candidate strategies to enhance the systemic anti-RCC immunity of GVAX can be considered. These include the coadministration of IL-2 to enhance basal antitumor immunity [3,5–7,32–34], allogeneic stem cell transplantation including nonmyeloablative stem cell transplantation to introduce allogeneic immunity [27], IL-12 or CD80 cDNA-transduced autologous tumor cells for the direct activation of CTLs, the blockade of CTLA-4/B7 interactions with monoclonal antibody to activate costimulation signals, and the functional activation of dendritic cells using HSP gp91 [35–38]. The administration of low-dose IL-2 as an anticancer immunotherapy has recently been introduced to decrease both the side effects and the cost of treatment [39–42].Our experience with three patients who were given GVAX followed by low-dose IL-2 would cast new light on anti-cancer immunotherapy, possibly by inducing tumor-specific immunity by GVAX, followed by enhancement of the broad antitumor immunity with systemic low-dose IL-2. In the present study, *in vitro* CTL analysis in these two patients supported the hypothesis that the antitumor CTL activity was maintained after administration of IL-2. The optimal duration of treatment with low-dose IL-2 in combination with GVAX remains to be determined by closely monitoring antitumor immunity both *in vitro* and *in vivo*.

Patients and Methods

Selection of Patients

The details of the study design and methods of vaccine production were essentially the same as those reported by Simons *et al.* [13,14], except for modifications that were implemented according to the regulations for

clinical gene therapy announced by the Japanese government between 1995 and 1997. Briefly, patients with stage IV RCC (Union Internationale Contre le Cancer classification of 1997) were eligible. Chemotherapy, radiotherapy, systemic IL-2- or interferon-α-based regimens, or other investigational agents were also offered as treatment options to these patients. The following eligibility criteria were used: primary RCC in place with evaluable metastasis after nephrectomy; Eastern Cooperative Oncology Group performance status of zero or one; appropriate surgical candidate and estimated life expectancy of at least 6 months; no major surgery, radiotherapy, chemotherapy, immunotherapy, or immunosuppressive medications within 1 month prior to enrollment; age >18 years; absence of active infection, i.e., WBC count <4000/μl, platelets <100,000/μl, total bilirubin <1.5 mg/dl, and creatinine <2.0 mg/dl; HIV seronegativity; and no history of autoimmune disease. The exclusion criteria included age <20 years; pregnant or lactating women; double malignant tumors; surgery; local or systemic treatment with corticosteroids; immunotherapy; irradiation or anti-cancer drugs 1 month before registration; leukocytosis of unknown origin; history of systemic lupus erythematosis, sarcoidosis, rheumatoid arthritis, autoimmune hemolytic anemia, autoimmune thyroiditis, glomerulonephritis, or vasculitis; apparent infection requiring treatment before second stage; apparent brain metastasis detected on CT scan or MRI; postnephrectomy deep vein thrombosis or pulmonary embolism that required treatment; and opium or alcohol abuse. The study was reviewed and approved by the Committee on Clinical Investigation and Institutional Gene Therapy Ethical Committee, The Institute of Medical Science, University of Tokyo, in April 1998, and by the Joint Committee of the BioScience Committees of the Ministry of Health, Labor, and Welfare and the Ministry of Education, Culture, Sports, Science, and Technology in August 1998.

Study Design

Patients were enrolled from September 1998 to May 2001. Eligible patients were nephrectomized after giving their initial informed consent. The second informed consent was obtained after safety confirmation tests, which included negative tests for microbial contaminants such as bacteria, fungi, mycoplasma, RCR, and endotoxin, and when sufficient production (>40 ng/10^6 cells/24 h) of GM-CSF was detected in the GM-CSF gene-transduced RCC. The vaccination schedule of GVAX, including additional vaccinations, is described precisely under Vaccine preparation and administration. Peripheral blood was obtained (as per NIH Recombinant DNA Advisory Committee and Food and Drug Administration guidelines) for detecting RCR before treatment, after vaccination, monthly for 3 months, every 3 months for the next 9months, and then yearly [14]. Long-term follow-up, including periodic evaluation for autoimmune disease and tumor progression, was performed.

Clinical Evaluation

The patients received daily physical examinations and periodic laboratory tests, which included hematological parameters and liver, renal, and immunological functions, prior to and after the vaccinations. The metastatic lesion volumes were measured using CT (lung, liver, bone, brain), MRI (liver, bone, brain), and thallium or technetium scintigraphy (whole body). Unenhanced helical CT images that covered each lesion were obtained during a single breath-hold. The thickness of the slices ranged from 3 to 10 mm, depending on the lesion size. The data were transferred to a workstation (Advantage Windows; General Electric Medical Systems, Milwaukee, WI, USA) to calculate the tumor volumes. Low-density areas, which represent lung parenchyma, were excluded at a threshold of −400 HU, and lesion sections were selected manually from the remaining areas of each slice. The lesion volume was calculated with a 3-D utility on the workstation for Cases 1, 2, and 3. The lesion in Case 4 was calculated as the sum of the perpendicular diameters of all lesions measured by CT scan, due to difficulties in measuring small multiple tumors volumetrically.

Vaccine Preparation and Administration

The methods used for autologous RCC vaccine preparation and MFGS-GM-CSF gene transfer at the Clinical Cell Processing Facility of the Institute of Medical Science Hospital at the University of Tokyo have been described previously [13]. The procedure complied with good manufacturing practices. Primary cultures were established and transduced at the first passage. Following *in vitro* expansion, the vaccine cells were irradiated at 150 Gy to prevent clonogenic survival *in vivo* after vaccination. GM-CSF production was determined using a GM-CSF ELISA kit (R&D Systems, Minneapolis, MN, USA) according to the manufacturer's instructions. Genomic integration of the GM-CSF cDNA into the patients' autologous RCC cells was determined by the standard Southern blotting method using MFG-GM-CSF plasmid DNA to determine the copy number, as described elsewhere [43]. The tests for microbial contaminants, i.e., bacteria, fungi, mycoplasma, RCR, and endotoxin, were all performed by BioReliance Corp. (Rockville, MD, USA). The vaccine cells were stored in liquid nitrogen until use. On the day of vaccination, 4×10^7 viable cells were administered intradermally in the first injection, and thereafter, 2×10^7 cells were administered at least five times at 2-week intervals, which was considered to be a superior vaccination schedule as described by Soiffer *et al.* [16]. Each patient was carefully screened for eligibility according to the inclusion criteria by the Institutional Review Board (IRB) of the Institute of Medical Science, University of Tokyo. The IRB permitted additional

administration of vaccine every 2 weeks when the yield of cells was higher than the 1.4×10^8 cells required for the six scheduled administrations and in cases in which the patient's physical condition was acceptable after further informed consent was obtained. The vaccinated sites were biopsied for microscopic examination at 3 and/or 7 days after every second vaccination.

Toxicity Assessment and Pharmacokinetic Analysis of Serum GM-CSF Levels

The levels of toxicity were graded using the National Cancer Institute's cancer common toxicity criteria for clinical trials. Toxicities were identified by medical history, physical examination, and review of the laboratory studies performed. Patients' sera were frozen in 1-ml aliquots at −80°C until the day of testing. The serum GM-CSF levels were determined for all collection time points by enzyme-linked immunosorbent assay using the Biotrak human GM-CSF ELISA system (Amersham International Plc., Amersham, UK) according to the manufacturer's protocol.

Histological Studies

Six-millimeter punch biopsies were removed from the intradermal injection sites on days 3 and/or 7 following the first vaccination. Prevaccination skin biopsies were obtained for comparison. Similarly, skin biopsies were also taken for evaluation of the DTH reaction 48 h after intradermal inoculation of RCC cells and NRC. Surgically removed and autopsy materials were used for the histological evaluation of tumors and tumor-infiltrating cells. Biopsy materials were fixed in 10% buffered formalin, embedded in paraffin, stained with H&E, and labeled with antibodies to CD3, BMP (rabbit antiserum to human myelin basic protein; DAKO Corp., Carpinteria, CA, USA), AE1/AE3 (pooled mAbs to human epithelial keratin, IgG1 subtype; Boehringer Mannheim, Indianapolis, IN, USA), S100 (rabbit anti-cow S100; DAKO), CD68 (anti-human macrophage CD68 mAb, IgG3-subtype; DAKO), HLA-DR (clone LN3, IgG2a subtype; Lab Vision Corp., Fremont, CA, USA), CD3 (clone PS1, mAb, IgG2a subtype; Novocastra Laboratories, Newcastle, UK), CD4 (clone 1F6, mAb, IgG1 subtype; Novocastra Laboratories), CD8 (clone 1A5, IgG1 subtype; Novocastra Laboratories), and CD20cy (B cell marker, clone L26, mAb, IgG2a subtype; Lab Vision Corp.). For the evaluation of tumor apoptosis, the TdT-mediated dUTP–biotin nick end-labeling (TUNEL) method was applied using an ApopTag Kit (Intergen Co., Purchase, NY, USA).

Delayed-Type Hypersensitivity Testing

To evaluate the cell-mediated immunity status of each patient before and after treatment, DTH testing was performed using seven common recall antigens (Multitest CMI; Connaught Laboratories, Swiftwater, PA, USA) according to the manufacturer's instructions. Reaction scoring was also performed according to the manufacturer's instructions. The patients were tested simultaneously for reactivity to autologous, irradiated cultured RCC cells and NRC. The autologous RCC cells and NRC for DTH testing were prepared and stored in liquid nitrogen according to the same procedure used for vaccine cell production omitting GM-CSF transduction. During storage, sterility testing for bacteria, fungi, mycoplasma, and endotoxin was carried out at the Department of Laboratory Medicine, Institute of Medical Science, University of Tokyo. PBMC were isolated using the standard Lymphoprep (d = 1.077; Nycomed Pharma AS, Oslo, Norway) density gradient centrifugation method. These cells were washed three times with HBSS, counted, and injected intradermally at 10^6 cells/0.2 ml. DTH reactions were observed 48 h after each DTH injection, i.e., 1 week before the first vaccination and 1 week after the second, fourth, and sixth vaccinations in all four patients.

Tumor Tissues, Peripheral Blood, and Skin Biopsies from Patients

Single-cell suspensions of tumor tissues were obtained from biopsied or autopsied (Case 1) tumor specimens that were minced mechanically and treated with collagenase and DNase. RCC cells and TILs were separated by density gradient centrifugation, as described elsewhere [24]. Heparinized peripheral blood samples (20 ml) were drawn from patients every other week before vaccination. For follow-up, samples were also drawn when the patients permitted. Patients' sera were frozen at −80°C until use for Western blot analysis. PBMC were isolated as above. PBMC and TIL (5×10^6 cells/tube) were cryopreserved using a programmable freezer and stored in liquid nitrogen. In addition, the cell pellets were frozen in liquid nitrogen until used for RNA extraction. Skin biopsies obtained from the DTH reaction site (6 mm in diameter) were cut into pieces measuring approximately 1 × 1 mm and rapidly frozen in liquid nitrogen until used for RNA extraction.

Assessment of Lymphocyte Proliferation and Cytokine Production

On the day of the assay, the cryopreserved samples were thawed. PBMC (1×10^5 cells/well) were cultured in the presence of irradiated (150 Gy) GM-CSF-transduced autologous tumor cells (1×10^4 cells/well) plus IL-2 (40 U/ml), in 96-well flat-bottomed plates. RPMI 1640 medium with L-glutamine (Invitrogen, Carlsbad, CA, USA) supplemented with 10% fetal bovine serum (BioWhittaker, Walkersville, MD, USA) and gentamicin was used as complete medium. On day 3 or 6, culture supernatants (100 μl/well) were collected from each well to determine the cytokine levels, and fresh medium was added. The cultures were then pulsed with [^{3}H]thymidine (0.5 μCi/well; DuPont-NEN, Boston, MA, USA) for a final 18 h and harvested on a Micro 96 harvester (Skatron, Lier, Norway), and the incorporated radioactivity was measured using a

microplate counter (Micro Beta Plus; Wallac, Turku, Finland). ELISAs for human IFN-γ, IL-5, and IL-10 were performed using ELISA kits (OptEIA; BD-Biosciences, Boston, MA, USA) according to the manufacturer's protocols.

Cytotoxicity Assay

To prepare effector cells, cultures with IL-2 and irradiated GM-CSF-transduced autologous tumor cells as described above were prepared in 96-well round-bottomed plates and the plates were cultured for 7 days. On the day of the assay, aliquots of 100 μl of the culture medium were removed from each well and then labeled target cells (5×10^3 cells/100 μl/well) were added. To label the target cells, single-cell suspensions of cultured autologous or allogeneic RCC cells, autologous NRC, and K562 cells were incubated with $Na_2^{51}CrO_4$ (100 μCi) for 1 h at 37°C and washed three times prior to use. For blocking experiments, F(ab′)2 anti-CD3 mAb prepared as described previously [44] was added to a final concentration of 10 μg/ml at the start of the assay. The plates were incubated at 37°C for 6 h, the supernatants were collected using a Skatron cell harvester system (Diversified Equipment Co., Lorton, VA, USA), and the radioactivity was measured using a γ counter. Spontaneous release (SR) and maximal release (MR) were measured in the supernatant of target cells alone with 100 μl of either medium or 10% Triton X-100 (Sigma, St. Louis, MO, USA). The percentage specific cytotoxicity was calculated using the following formula: % cytotoxicity = experimental release − SR/MR − SR × 100.

Analysis of the TCR β Repertoire

Total RNA was isolated from PBMC and homogenized tumor tissues using Trizol reagent (Invitrogen) with a cryo-press crusher (Microtech Nichion, Tokyo, Japan). TCR β repertoire analysis was performed as described previously [45]. Briefly, TCR β cDNA was synthesized using C-oligonucleotides (5′-CGGGCTGCTCCTT GAGGGGCTGCG-3′) with AMV reverse transcriptase (Invitrogen). The TCR cDNA was amplified by 40 cycles of PCR with each of the 24 Vβ 5′ primers (Vβ 1-w24) and the Cβ 3′ primer in PCR buffer containing 1 U of Hot Start *Taq* polymerase (AmpliTaq Gold; Applied Biosystems, Foster City, CA, USA). The products were subjected to Southern blot analysis using a ^{32}P-labeled Cβ probe. Different samples of each Vβ product were compared after quantifying the autoradiographs by densitometry BAS-2000II (Fuji Photo Film Corp.). To refine CDR3 size analysis, the Vβ–Cβ PCR product was copied in a 10-cycle run-off reaction with a fluorescence-labeled Cβ primer. The labeled PCR products were electrophoresed on a DNA sequencer (ABI Prism 377; Applied Biosystems) in the presence of a fluorescent size standard and analyzed with a DNA fragment size program (GeneScan; Applied Biosystems).

The PCR products of the CDR3 fragment were cloned into the pCRII-TOPO vector system (Invitrogen). Thirty colonies containing the insert fragment were selected at random and sequenced using an ABI Prism Cycle Sequencing Kit (Applied Biosystems) and an automatic DNA sequencer ABI 373 (Applied Biosystems). The amino acid sequence of the CDR3 region was deduced using the software GENETYX-MAC v10.1.4 (Software Development Co., Ltd., Tokyo, Japan).

Detection of Antitumor Antibodies

The antitumor antibodies appearing in patients' sera were detected by Western blot analysis according to the standard procedure with some modifications [18]. Briefly, humoral antitumor immune responses were evaluated using the reactivity of the tumor cell lysate and sera from the patients. Autologous RCC and NRC were extracted in lysis buffer containing 20 mM Tris–HCl at pH 7.6, 1% NP-40, 150 mM NaCl, 1 mM phenylmethylsulfonyl fluoride, and 500 units/ml aprotinin (Calbiochem, La Jolla, CA, USA). A fibroblast cell line of human lip origin, which was established in our laboratory, and a small-cell lung carcinoma cell line, H69, were used as irrelevant control cells. Cell lysates were denatured, reduced in SDS sample buffer with 2-mercaptoethanol, and then electrophoresed on 7.5% polyacrylamide minigels (Bio-Rad Laboratories, Hercules, CA, USA). The proteins were transferred onto Immobilon membranes (Millipore, Bedford, MA, USA) and the blots were stained with Ponceau S solution (Sigma) for visualization. After destaining with TBST (0.1% Tween 20–Tris-buffered saline) and blocking with 5% nonfat dried milk in TBST overnight, the blots were probed with diluted (1:300) patient sera for 2 h. Horseradish peroxidase-conjugated rabbit F(ab′)2 anti-IgG Ab (DAKO, 1:3000 dilution) was added for 1 h, and the blots were developed with an ECL kit (Amersham Biosciences, Piscataway, NJ, USA).

Acknowledgments

We thank Drs. Fumihiko Komine, Tsuyoshi Tanabe, Hitomi Nagayama, Hitoshi Hibino, Muneomi Endo, Tomoko Yamazaki, Mariko Morishita, Koichiro Kuwabara, Momoyo Ohki, Sanae Suzuki, and the staff of The Advanced Clinical Research Center, Research Hospital, The Institute of Medical Science, University of Tokyo, for their excellent patient care and their strong support of this clinical study. We also thank Drs. Ken-ichi Tobisu and Hiroyuki Fujimoto (National Cancer Center, Japan), Taro Shuin (Kochi Medical College), Shunichi Fukuhara (Kyoto University), Yusuke Nakamura (The Institute of Medical Science, University of Tokyo), Toshio Kuroki (Gifu University), Ken-ichi Arai (The Institute of Medical Science, University of Tokyo), Jonathan W. Simons (Emory University), and Glenn Dranoff (Dana-Farber Cancer Institute) for helpful advice and discussions. This work was supported by grants from the Ministry of Health, Labor, and Welfare and the Ministry of Education, Culture, Sports, Science, and Technology, Japan.

RECEIVED FOR PUBLICATION JULY 5, 2004; ACCEPTED JULY 5, 2004.

References

1. Marumo, K., *et al.* (2001). The prevalence of renal cell carcinoma: nation-wide survey in Japan in 1997. *Int. J. Urol.* 8: 359–365.
2. Medical Research Council Renal Cancer Collaborators Interferon-α and survival in

doi:10.1016/j.ymthe.2004.07.001

metastatic renal carcinoma: early results of a randomized controlled trial. *Lancet* **353:** 14–17.
3. Bukowski, R. M. (1997). Natural history and therapy of metastatic renal cell carcinoma. *Cancer* **80:** 1198–1220.
4. Motzer, R. J., Bacik, J., Murphy, B. A., Russo, P., and Mazumdar, M. (2002). Interferon-α as a comparative treatment for clinical trials of new therapies against advanced renal cell carcinoma. *J. Clin. Oncol.* **20:** 289–296.
5. Clark, J. I., *et al.* (1999). Daily subcutaneous ultra-low-dose interleukin 2 with daily low-dose interferon-α in patients with advanced renal cell carcinoma. *Clin. Cancer Res.* **5:** 2374–2380.
6. Tagliaferri, P., *et al.* (1998). Daily low-dose subcutaneous recombinant interleukin-2 by alternate weekly administration. *Am. J. Clin. Oncol.* **21:** 48–53.
7. Figlin, R. A., *et al.* (1999). Multicenter, randomized, phase III trial of $CD8^+$ tumor-infiltrating lymphocytes in combination with recombinant interleukin-2 in metastatic renal cell carcinoma. *J. Clin. Oncol.* **17:** 2521–2529.
8. Childs, R., *et al.* (2000). Regression of metastatic renal-cell carcinoma after non-myeloablative allogeneic peripheral-blood stem-cell transplantation. *N. Engl. J. Med.* **343:** 750–758.
9. Dranoff, G., *et al.* (1993). Vaccination with irradiated tumor cells engineered to secrete murine granulocyte-macrophage colony-stimulating factor stimulates potent, specific, and long-lasting anti-tumor immunity. *Proc. Natl. Acad. Sci. USA* **90:** 3539–3543.
10. Jaffee, E. M., Thomas, M. C., Huang, A. Y. C., Hauda, K. M., Levitsky, H. I., and Pardoll, D. M. (1996). Enhanced immune priming with spatial distribution of paracrine cytokine vaccines. *J. Immunother.* **19:** 176–183.
11. Dranoff, G. (2002). GM-CSF-based cancer vaccines. *Immunol. Rev.* **188:** 147–154.
12. Ellem, K. A., *et al.* (1997). A case report: immune responses and clinical course of the first human use of granulocyte/macrophage-colony-stimulating-factor-transduced autologous melanoma cells for immunotherapy. *Cancer Immunol. Immunother.* **44:** 10–20.
13. Berns, A. J., *et al.* (1995). Phase I study of non-replicating autologous tumor cell injections using cells prepared with or without GM-CSF gene transduction in patients with metastatic renal cell carcinoma. *Hum. Gene Ther.* **6:** 347–368.
14. Simons, J. W., *et al.* (1997). Bioactivity of autologous irradiated renal cell carcinoma vaccines generated by ex vivo granulocyte-macrophage colony-stimulating factor gene transfer. *Cancer Res.* **57:** 1537–1546.
15. Simons, J. W., *et al.* (1999). Induction of immunity to prostate cancer antigens: results of a clinical trial of vaccination with irradiated autologous prostate tumor cells engineered to secrete granulocyte-macrophage colony-stimulating factor using ex vivo gene transfer. *Cancer Res.* **59:** 5160–5168.
16. Soiffer, R., *et al.* (1998). Vaccination with irradiated autologous melanoma cells engineered to secrete human granulocyte-macrophage colony-stimulating factor generates potent antitumor immunity in patients with metastatic melanoma. *Proc. Natl. Acad. Sci. USA* **95:** 13141–13146.
17. Chang, A. E., Li, Q., Bishop, D. K., Normolle, D. P., Redman, B. D., and Nickoloff, B. J. (2000). Immunogenic therapy of human melanoma utilizing autologous tumor cells transduced to secrete granulocyte-macrophage colony-stimulating factor. *Hum. Gene Ther.* **11:** 839–850.
18. Jaffee, E. M., *et al.* (2001). Novel allogeneic granulocyte-macrophage colony-stimulating factor-secreting tumor vaccine for pancreatic cancer: a phase I trial of safety and immune activation. *J. Clin. Oncol.* **19:** 145–156.
19. Kusumoto, M., *et al.* (2001). Phase 1 clinical trial of irradiated autologous melanoma cells adenovirally transduced with human GM-CSF gene. *Cancer Immunol. Immunother.* **50:** 373–381.
20. Salgia, R., *et al.* (2003). Vaccination with irradiated autologous tumor cells engineered to secrete granulocyte-macrophage colony-stimulating factor augments antitumor immunity in some patients with metastatic non-small-cell lung carcinoma. *J. Clin. Oncol.* **21:** 624–630.
21. Soiffer, R., *et al.* (2003). Vaccination with irradiated, autologous melanoma cells engineered to secrete granulocyte-macrophage colony-stimulating factor by adeno-viral-mediated gene transfer augments antitumor immunity in patients with metastatic melanoma. *J. Clin. Oncol.* **21:** 3343–3350.
22. Nemunaitis, J., *et al.* (2004). Granulocyte-macrophage colony-stimulating factor gene-modified autologous tumor vaccines in non-small-cell lung cancer. *J. Natl. Cancer Inst.* **96:** 326–331.
23. Tani, K., *et al.* (2000). Progress reports on immune gene therapy for stage IV renal cell carcinoma using lethally irradiated granulocyte-macrophage colony-stimulating factor-transduced autologous renal cancer cells. *Cancer Chemother. Pharmacol.* **46**(Suppl.): S73–S76.
24. Kawai, K., *et al.* (2002). Advanced renal cell carcinoma treated with granulocyte-macrophage colony-stimulating factor gene therapy: a clinical course of the first Japanese experience. *Int. J. Urol.* **9:** 462–466.
25. Thomas, M. C., Greten, T. F., Pardoll, D. M., and Jaffee, E. M. (1998). Enhanced tumor protection by granulocyte-macrophage colony-stimulating factor expression at the site of an allogeneic vaccine. *Hum. Gene Ther.* **9:** 835–843.
26. Borrello, I., Sotomayor, E. M., Cooke, S., and Levitsky, H. I. (1999). A. universal granulocyte-macrophage colony-stimulating factor-producing bystander cell line for use in the formation of autologous tumor cell-based vaccines. *Hum. Gene Ther.* **10:** 1983–1991.
27. Luznik, L., *et al.* (2003). Successful therapy of metastatic cancer using tumor vaccines in mixed allogeneic bone marrow chimeras. *Blood* **101:** 1645–1652.
28. Mastrangelo, M. J., *et al.* (1999). Intratumoral recombinant GM-CSF-encoding virus as gene therapy in patients with cutaneous melanoma. *Cancer Gene Ther.* **6:** 409–422.
29. Hanada, K. -I., Yewdell, J. W., and Yang, J. C. (2004). Immune recognition of a human renal cancer antigen through post-translational protein splicing. *Nature* **427:** 252–256.
30. Puisieux, I., *et al.* (1996). Restriction of the T-cell repertoire in tumor-infiltrating lymphocytes from nine patients with renal-cell carcinoma: relevance of the CDR3 length analysis for the identification of in situ clonal T-cell expansions. *Int. J. Cancer* **66:** 201–208.
31. Gaudin, C., *et al.* (1995). In vivo local expansion of clonal T cell subpopulations in renal cell carcinoma. *Cancer Res.* **55:** 685–690.
32. Gaugler, B., *et al.* (1996). A new gene encoding for an antigen recognized by autologous cytolytic T lymphocytes on a human renal carcinoma. *Immunogenetics* **44:** 323–330.
33. Vissers, J. L. M., *et al.* (1999). The renal cell carcinoma-associated antigen G250 encodes a human leukocyte antigen (HLA)-A2.1-restricted epitope recognized by cytotoxic T lymphocytes. *Cancer Res.* **59:** 5554–5559.
34. Rosenberg, S. A., *et al.* (1987). A progress report on the treatment of 157 patients with advanced cancer using lymphokine-activated killer cells and interleukin-2 or high-dose interleukin-2 alone. *N. Engl. J. Med.* **316:** 889–895.
35. Nakazaki, Y., *et al.* (1998). Vaccine effect of granulocyte-macrophage colony-stimulating factor or CD80 gene-transduced murine leukemia/lymphoma cells and their cooperative enhancement of antitumor immunity. *Gene Ther* **5:** 1355–1362.
36. Wang, Z., Qiu, S. J., Ye, S. L., Tang, Z. Y., and Xiao, X. (2001). Combined IL-12 and GM-CSF gene therapy for murine hepatocellular carcinoma. *Cancer Gene Ther.* **8:** 751–758.
37. Van Elasas, A., Hurwitz, A. A., and Allison, J. P. (1999). Combination immunotherapy of B16 melanoma using anti-cytotoxic T lymphocyte-associated antigen 4 (CTLA-4) and granulocyte/macrophage colony-stimulating factor (GM-CSF)-producing vaccines induces rejection of subcutaneous and metastatic tumors accompanied by auto-immune depigmentation. *J. Exp. Med.* **190:** 355–366.
38. Kojima, T., *et al.* (2003). Tumor-derived Gp96 combined with GM-CSF gene-transduced tumor cells inhibit tumor growth in mice through migration and maturation of $CD11c^+$ cells. *Hum. Gene Ther.* **14:** 715–728.
39. Buzio, C., *et al.* (1997). Effectiveness of very low doses of immunotherapy in advanced renal cell cancer. *Br. J. Cancer* **76:** 541–544.
40. Lissoni, P., *et al.* (2002). Ten-year survival results in metastatic renal cell cancer patients treated with monoimmunotherapy with subcutaneous low-dose interleukin-2. *Anticancer Res.* **22:** 1061–1064.
41. Schomburg, A., *et al.* (1992). In vivo and ex vivo antitumor activity in patients receiving low-dose subcutaneous recombinant interleukin-2. *Nat. Immunol.* **11:** 133–143.
42. Sobol, R. E., *et al.* (1999). Interleukin 2 gene therapy of colorectal carcinoma with autologous irradiated tumor cells and genetically engineered fibroblasts: a phase I study. *Clin. Cancer Res.* **5:** 2359–2365.
43. Tani, K., *et al.* (1989). Implantation of fibroblasts transfected with human granulocyte colony-stimulating factor (G-CSF) cDNA into mice as a model of cytokine supplement gene therapy. *Blood* **74:** 1274–1280.
44. Azuma, M., Cayabyab, M., Buck, D., Phillips, J. H., and Lanier, L. L. (1992). CD28 interaction with B7 costimulates primary allogeneic proliferative responses and cytotoxicity mediated by small, resting T lymphocytes. *J. Exp. Med.* **175:** 353–360.
45. Hase, H., *et al.* (2000). Case report: the availability of TCR-Vβ repertoires analysis with RT-PCR methods for the early detection of pulmonary relapsed T-cell malignancy after the autologous stem cell transplantation. *Am. J. Hematol.* **64:** 124–127.

Available online at www.sciencedirect.com

SCIENCE DIRECT

European Journal of Pharmacology 502 (2004) 265–270

www.elsevier.com/locate/ejphar

Inhibitory effect of low-dose estrogen on neointimal formation after balloon injury of rat carotid artery

Tokumitsu Watanabe[a], Yukiko Miyahara[a], Masahiro Akishita[b], Takashi Nakaoka[c], Naohide Yamashita[c], Katsuya Iijima[a], Hong Kim[a], Koichi Kozaki[a], Yasuyoshi Ouchi[a,*]

[a]*Department of Geriatric Medicine, Graduate School of Medicine, University of Tokyo, 7-3-1 Hongo, Bunkyo-ku, Tokyo 113-8655, Japan*
[b]*Department of Geriatric Medicine, Kyorin University School of Medicine, Tokyo 181-8611, Japan*
[c]*Department of Advanced Medicine, Institute of Medical Science, University of Tokyo, Tokyo 108-8639, Japan*

Received 11 March 2004; received in revised form 16 July 2004; accepted 1 September 2004
Available online 27 September 2004

Abstract

The current regimens of hormone replacement therapy for postmenopausal women, estrogen combined with progestogen, have failed to show beneficial effects for the prevention of atherosclerotic disease. Although the relatively higher dose of estrogen contained in those regimens exerted adverse effects, there are few data examining a lower dose of estrogen in an atherosclerosis model. Therefore, we investigated experimentally whether lower doses of estrogen could inhibit neointimal formation after balloon injury of the rat carotid artery. Ten-week-old Wistar rats were subjected to ovariectomy or sham-operation (n=7). Four days after ovariectomy, rats were implanted with an osmotic mini-pump containing 17-β estradiol (0.2, 1, 2, 10 and 20 μg/kg/day; n=6, 4, 8, 6 and 5, respectively) or placebo (n=10). After 3 days of hormone therapy, balloon injury was performed in the left common carotid artery. Neointimal formation was histologically evaluated 2 weeks after injury. Cross-sectional intimal area and the ratio of intimal area to medial area were dose-dependently reduced by estrogen replacement compared with those in ovariectomized rats without estrogen replacement. The effects of estrogen replacement were identical to those of an angiotensin II type 1 receptor blocker, candesartan. Interestingly, the effect was significant even in rats receiving lower doses of estrogen, in which plasma estradiol concentrations were not increased and the hyperplastic response of the uterus was minimal. These results suggest the efficacy of low-dose estrogen therapy for the protection of atherosclerosis.

Keywords: Estrogen; Low-dose; Neointimal formation

1. Introduction

Previous studies have shown that estrogen administration in ovariectomized animals inhibits the process of atherosclerosis. Different doses of estrogens in combination with or without progestins have decreased the lesion formation in injured vessels or cholesterol-fed animals using rodents, rabbits and swine (Chen et al., 1996; Oparil et al., 1997; Bakir et al., 2000; Chandrasekar and Tanguay, 2000; Finking et al., 2001; Tolbert et al., 2001). Most of the studies, however, have used the estradiol doses of 20 μg/kg/day or higher, which were accompanied by the raised plasma estradiol concentration compared to intact female animals (Chen et al., 1996; Bakir et al., 2000; Tolbert et al., 2001). More importantly, these doses of estrogen (≥20 μg/kg/day of estradiol subcutaneously) elicited adverse effects such as uterine hyperplasia (Bakir et al., 2000; Tolbert et al., 2001; Xu et al., 2003) and dyslipidemia (Joles et al., 1998; Gades et al., 1998; Tomiyoshi et al., 2002). On the other hand, it has been reported that the effect of estradiol on uterine weight was dose-dependent (Kordelhuc and Jolette, 2002) and that low dose estrogen (approximately 3 μg/kg/day of estradiol) could exert its favorable effect on bone metabolism (Chen et al., 2001). Since limited information is

* Corresponding author. Tel.: +81 3 5800 8830; fax: +81 3 5800 6530.
E-mail address: youchi-tky@umin.ac.jp (Y. Ouchi).

0014-2999/$ - see front matter © 2004 Elsevier B.V. All rights reserved.
doi:10.1016/j.ejphar.2004.09.011

available on the vascular effect of low dose estrogen therapy, it is intriguing to study whether the lower dose of estrogen could inhibit vascular lesion formation.

In the present study, we hypothesized that lower doses of estrogen could have protective effects on the process of atherosclerosis with minimal adverse effects. To test this hypothesis, we examined neointimal formation of the carotid artery after balloon angioplasty in ovariectomized female rats receiving 10 μg/kg/day or lower doses of estradiol.

2. Materials and methods

2.1. Animals

Ten-week-old female Wistar rats (Oriental Yeast, Tokyo) were used in this study. They were housed in individual cages in a room in which lighting was controlled (12 h on, 12 h off) and room temperature was kept at ≈22 °C. They were given a standard diet and water ad libitum. All the surgical procedures were performed under sterile conditions. All of the experimental protocols were approved by the Animal Research Committee of the University of Tokyo.

2.2. Experimental protocols

Rats were randomly divided into 10 groups. Nine groups of rats were subjected to ovariectomy and the other group underwent sham operation (Akishita et al., 1997). After a 4-day recovery period, six groups of ovariectomized rats were subcutaneously implanted with osmotic minipumps (Alzet 2002, 0.5 μl/h; Alza) prefilled with water-soluble 17β-estradiol (0.2, 1, 2, 10 or 20 μg/kg/day; Sigma) or its vehicle (2-hydroxypropyl-β-cyclodextrin; Sigma) under ether anesthesia. To compare the effect of estrogen with that of an angiotensin II type 1 (AT1) receptor blocker, candesartan, the remaining four groups of rats were subcutaneously implanted with an osmotic minipump containing the active metabolite of candesartan, candesartan cilexetil (2, 20 or 200 μg/kg/day; kindly donated by Takeda Chemical Industries, Tokyo) or its vehicle (0.9% saline).

Three days after minipump implantation, balloon injury was performed as previously described (Chen et al., 1996; Nakaoka et al., 1997). General anesthesia was induced by the administration of 90 mg/kg of ketamine intraperitoneally and 15 mg/kg of xylazine intramuscularly. The left carotid artery was exposed and its branches were ligated using 7–0 nylon. After intravenous injection of 75 U/kg of heparin, a portion of the external carotid artery and a portion of the internal carotid artery were cross-clipped using a microclip (2v-clip: S&T, Neuhausen, Switzerland). A 2F Fogarty embolectomy catheter (Baxter, Irvine, CA) was introduced into the artery via the external carotid artery. The common carotid artery was injured by six passes of an embolectomy catheter inflated with 0.2 ml of air. The portion proximal to the incision was ligated with 7–0 nylon, the cross-clip was released and the common carotid artery was reperfused.

2.3. Measurement of hormones and lipids

Blood sampling was performed at sacrifice, after a 16-h overnight fast, to measure serum concentrations of estradiol and progesterone, serum lipids and other biochemical parameters. Serum estradiol, estrone and progesterone concentrations were measured by sensitive radioimmunoassay (Hashimoto et al., 2002). Serum total cholesterol and triglyceride concentrations were measured enzymatically, and serum high-density lipoprotein cholesterol concentration was measured by heparin-Ca^{2+} Ni^{2+} precipitation method (Hashimoto et al., 2002).

2.4. Morphometrical analysis of the balloon-injured carotid artery

A portion of the left common carotid artery was harvested at 14 days after balloon injury. The artery was perfusion- and pressure-fixed at 100 mm Hg using 10% neutral formalin buffer and then paraffin-embedded. Five round cross-sections per 1.5-cm length of artery specimens were stained with *Elastica van Gieson staining*, and photographed. Cross-sectional areas of the intima and the media were measured using an image analyzing software package (Scion Image, shared NIH software). The average of five sections was used for analysis as the value of each animal.

2.5. Data analysis

Values are expressed as mean±S.E.M. in the text, table and figures. Data were analyzed by one-factor analysis of variance (ANOVA) followed by Newman–Keuls' multiple comparison test. Differences with a value of $P<0.05$ were considered statistically significant.

3. Results

Sixty-five rats were set up and allocated to each group. Four rats were excluded because of failure of intervention. Estrogen replacement in ovariectomized rats increased serum concentration of estradiol dose-dependently, and replacement of 2 μg/kg/day estradiol achieved a concentration comparable to that in sham-operated rats (Table 1). In all groups, the serum concentration of estrone was below the detection limit (data not shown) and that of progesterone was unchanged. With respect to the lipid profile, the concentration of total cholesterol, triglyceride and high-density lipoprotain (HDL) cholesterol were increased in rats

Table 1
Blood pressure, serum lipids, plasma hormone concentrations and body and uterus weight after balloon injury of left carotid arteries of female Wistar rats

	Sham	Ovariectomy+17β-estradiol (μg/kg/day)						Ovariectomy+TCV-116 (μg/kg/day)		
		0	0.2	1	2	10	20	0	2	20
No. of rats	7	10	6	4	8	6	5	4	4	4
SBP (mm Hg)	121±4	113±7	123±2	120±5	127±2	121±4	121±4	121±7	122±7	116±8
T.chol (mg/dl)	76±9	75±5	86±4	78±10	84±6	96±5[a]	113±3[b]	79±2	89±4	81±8
HDL-C (mg/dl)	20±2	21±3	20±2	16±3	23±2	27±1	30±1[a]	17±2	21±2	22±2
Triglyceride (mg/dl)	41±6	53±8	46±9	64±16	91±13[a]	87±10[a]	153±31[b]	64±11	25±6	35±10
Estradiol (pg/ml)	19±4[b]	8±1	9±1	12±2	20±2[b]	54±5[b]	96±3[b]	11±3	11±1	14±2
Progesterone (ng/ml)	20±5	13±2	6±3	21±5	9±2	11±3	5±2	16±4	21±6	15±6
Body weight (g)	269±6	282±8	281±8	260±6	264±6	257±5[a]	263±7	285±10	290±5	290±3
Uterus (mg)	661±102[b]	174±29	321±23	577±46[b]	511±76[b]	–	–	148±22	149±5	156±7

Values are expressed as mean±S.E.M. SBP, systolic blood pressure; T.chol, total cholesterol; HDL-C, high-density lipoprotein cholesterol; –, not examined.
[a] $P<0.05$ vs. OVX+0 μg/kg/day of 17β-estradiol.
[b] $P<0.01$ vs. OVX+0 μg/kg/day of 17β-estradiol.

receiving higher doses of estrogen, as previously reported (Gades et al., 1998; Joles et al., 1998; Tomiyoshi et al., 2002), whereas those were unchanged in rats receiving 2 μg/kg/day or a lower dose of estrogen. The body weight of rats treated with higher doses was significantly lower than that in rats without estrogen replacement. In contrast, uterine weight in rats receiving lower doses of estrogen was greater than that in rats without estrogen.

Morphometric analysis showed that the neointimal area of the carotid artery was dose-dependently decreased by estrogen replacement (Figs. 1 and 2). As shown in Fig. 2, neointimal formation was sufficiently attenuated even in rats treated with 0.2 μg/kg/day of estradiol compared to that in ovariectomized rats without estrogen replacement. The inhibitory effect of estrogen on neointimal formation was compared with that of candesartan because the effects of AT1 receptor blockers including candesartan have been established (Kim et al., 2002; Liu et al., 2002; Nozawa et al., 1999; Tazawa et al., 1999). The effect of 20 μg/kg/day estradiol was more potent than that of subdepressor dose of candesartan (20 μg/kg/day) and was as potent as that of 200 μg/kg/day candesartan; a dose that lowered blood pressure and body weight as well as neointimal formation (intima/media ratio was 0.66±0.07, data not shown). Importantly, the effect of 2 μg/kg/day or a lower dose of estradiol on neointima formation was comparable to that of 20 μg/kg/day candesartan (Fig. 2). Medial area was not different among all groups of rats. Small non-significant differences in several measurements between the control for estrogen and that for candesartan were likely to be due

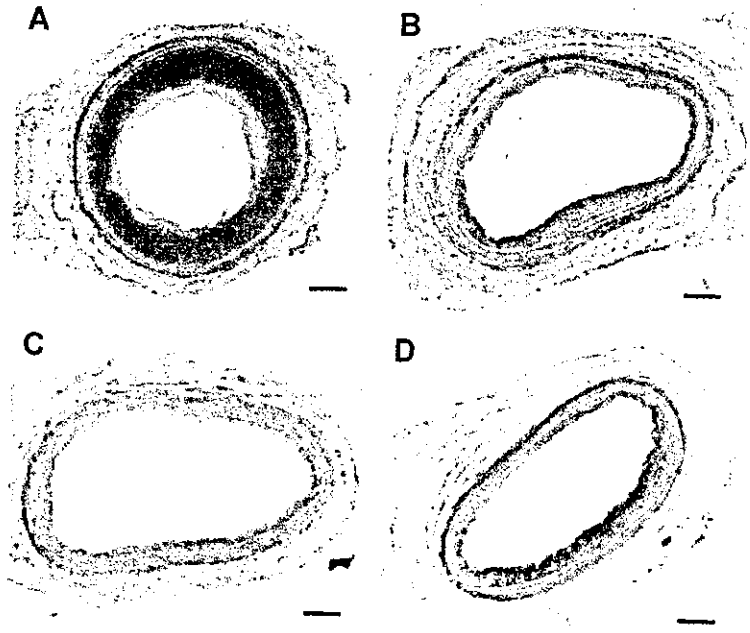

Fig. 1. Representative cross-sections of the rat carotid artery 2 weeks after balloon injury (elastica van gieson staining, magnification ×100). Rats were treated with 20% cyclodextrin vehicle (A), 0.2 μg/kg/day of 17-β estradiol (B), 20 μg/kg/day of 17-β estradiol (C) and 20 μg/kg/day of candesartan (D). Bars: 100 μm.

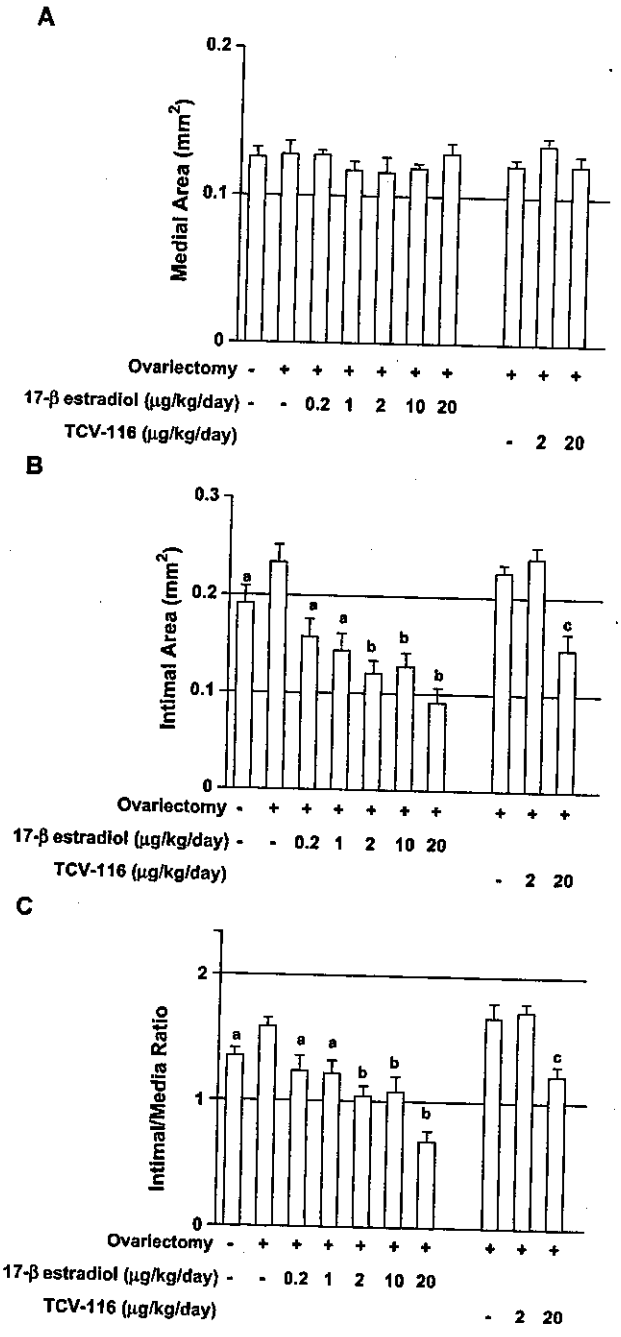

Fig. 2. Morphometric analyses of intimal area (A), medial area (B) and intima/media area ratio (C) in the carotid artery 2 weeks after balloon injury. The results are expressed as mean±S.E.M. $^{a}P<0.05$, $^{b}P<0.01$ vs. ovariectomized rats without 17-β estradiol, $^{c}P<0.01$ vs. ovariectomized rats without candesartan.

to the variation of the measurements rather than the effect of vehicle for each group.

4. Discussion

This study showed that subcutaneous administration of 2 μg/kg/day or lower doses of estradiol inhibited neointimal formation after vascular injury with minimal adverse effects on the uterus and lipid metabolism, suggesting the efficacy of lower doses of hormone replacement therapy for the prevention of atherosclerosis.

Estrogen has been reported to inhibit neointimal formation after vascular injury in rodents using balloon angioplasty of the rat carotid artery (Bakir et al., 2000; Chen et al., 1996; Oparil et al., 1997, 1999), cuff placement around the rat femoral artery (Akishita et al., 1997) and ligation of the mouse carotid artery (Tolbert et al., 2001). Oparil and her colleagues have shown using the rat carotid balloon-injury model that subcutaneous administration of 20 μg/kg/day estradiol reduced neointimal formation by more than 50% compared to that without estradiol treatment (Chen et al., 1996; Oparil et al., 1997, 1999; Bakir et al., 2000). In their studies, plasma estradiol levels in estrogen-replaced rats (135.0±5.7 pg/ml, Chen et al., 1996, or 32.0±4.8 pg/ml, Bakir et al., 2000) were higher than those in intact female rats (51.9±5.8 pg/ml, Chen et al., 1996, or 25±6.9 pg/ml, Bakir et al., 2000). In the present study, administration of 10 or 20 μg/kg/day estradiol in ovariectomized rats inhibited neointimal formation with the increased plasma estradiol concentration beyond that in sham-operated rats as well. These results suggest that the estradiol doses used in the previous studies (>10 μg/kg/day) may be relatively high although plasma estradiol concentration fluctuates in rats with the estrous cycle (ranged from 16±2 to 39±7 pg/ml, Anisimov and Okulov, 1980, or from 1±1 to 44±15 pg/ml, Hawkins et al., 1975), and changes with development and age (Meijs-Roelofs et al., 1975). In contrast, replacement of 2 μg/kg/day estradiol achieved serum estradiol concentrations comparable to those in sham-operated rats in the present study. Replacement of 1 μg/kg/day or a lower dose of estradiol did not increase the serum estradiol concentration. However, the inhibition of neointimal formation was significant at the lower doses and was comparable to the effect of 20 μg/kg/day of candesartan (Fig. 2). Moreover, 1 μg/kg/day or a lower dose of estradiol did not increase the serum triglyceride concentration, and 0.2 μg/kg/day of estradiol caused the minimal and non-significant increase of uterus weight. This could be a new finding with respect to the adverse effects on lipid profiles and uterus. Taken these findings together, a local effect of estrogen replacement on organs or cells was observed even if circulating estrogen was not elevated, providing some hints on determining the dose of hormone replacement therapy.

In the present study, we did not demonstrate the mechanisms by which estrogen inhibited neointimal formation. Previous reports have shown that re-endothelialization (White et al., 1997), preservation of endothelial survival (Sudoh et al., 2001) and function (White et al., 1997), inhibition of smooth muscle cell proliferation (Akishita et al., 1997) and inhibition of fibroblast proliferation and differentiation in the adventitia (Oparil et al., 1999) contribute to the effect of estrogen on the response to

vascular injury. Stimulation of nitric oxide synthesis as well as modulation of other vasoactive substances has been implicated in these effects, although activation of endothelial nitric oxide synthase may play a major role (Chambliss and Shaul, 2002). Further investigation is needed to elucidate the contribution and interaction of these factors in the effects of lower doses of estrogen on neointimal formation.

Recent randomized trials (Hulley et al., 1998; Rossouw et al., 2002) have suggested that hormone replacement therapy with the standard regimen should not be recommended for postmenopausal women. Improvement of the regimen, such as the dose, route (oral or subcutaneous) or schedule (continuous or cyclic), could resolve the adverse effects of hormone replacement therapy, although few data are currently available (Grodstein et al., 2000; Jick et al., 1996; Hashimoto et al., 2002; Wakatsuki et al., 2003, 2004). Direct comparisons of animal studies to clinical studies are inadequate because several major differences can be pointed including route of administration, duration of the treatment, cardiovascular risk profile of subjects and body fat distribution. However, our experimental result that lower doses of estrogen inhibited the response to vascular injury with relatively small adverse effects may imply the potential efficacy of low dose hormone replacement therapy in postmenopausal women.

Acknowledgments

This work was supported by grants from the Ministry of Education, Science, Sports and Culture of Japan (13557062, 15390239), by a Grant-in-Aid for Scientific Research from the Ministry of Health, Labor and Welfare of Japan (H13-Choju-016, H15-Choju-015), and, in part, by the Japan–China Sasakawa Medical Fellowship grant.

References

Akishita, M., Ouchi, Y., Miyoshi, H., Kozaki, K., Inoue, S., Ishikawa, M., Eto, M., Toba, K., Orimo, H., 1997. Estrogen inhibits cuff-induced intimal thickening of rat femoral artery: effects on migration and proliferation of vascular smooth muscle cells. Atherosclerosis 130, 1–10.

Anisimov, V.N., Okulov, V.B., 1980. Effect of ageing on concentration of estradiol in serum and the epidermal G2 chalone in vaginal mucosa of rats. Exp. Gerontol. 15, 87–91.

Bakir, S., Mori, T., Durand, J., Chen, Y.F., Thompson, J.A., Oparil, S., 2000. Estrogen-induced vasoprotection is estrogen receptor dependent: evidence from the balloon-injured rat carotid artery model. Circulation 101, 2342–2344.

Chambliss, K.L., Shaul, P.W., 2002. Estrogen modulation of endothelial nitric oxide synthase. Endocr. Rev. 23, 655–686.

Chandrasekar, B., Tanguay, J.F., 2000. Local delivery of 17-beta-estradiol decreases neointimal hyperplasia after coronary angioplasty in a porcine model. J. Am. Coll. Cardiol. 36, 1972–1978.

Chen, S.J., Li, H., Durand, J., Oparil, S., Chen, Y.F., 1996. Estrogen reduces myointimal proliferation after balloon injury of rat carotid artery. Circulation 93, 577–584.

Chen, J.L., Yao, W., Frost, H.M., Li, C.Y., Setterberg, R.B., Jee, W.S.S., 2001. Bipedal stance exercise enhances antiresorption effects of estrogen and counteracts its inhibitory effect on bone formation in sham and ovariectomized rats. Bone 29 (2), 126–133.

Finking, D., Krauss, N., Romer, S., Eckert, S., Lenz, C., Kamenz, J., Menke, A., Brehme, U., Hanke, H., 2001. 17beta-estradiol, gender independently, reduces atheroma development but not neointimal proliferation after balloon injury in the rabbit aorta. Atherosclerosis 154, 39–49.

Gades, M.D., Stern, J.S., van Goor, H., Nguyen, D., Johnson, P.R., Kaysen, G.A., 1998. Estrogen accelerates the development of renal disease in female obese Zucker rats. Kidney Int. 53, 130–135.

Grodstein, F., Manson, J.E., Colditz, G.A., Willett, W.C., Speizer, F.E., Stampfer, M.J., 2000. A prospective, observational study of postmenopausal hormone therapy and primary prevention of cardiovascular disease. Ann. Intern. Med. 133, 933–941.

Hashimoto, M., Miyao, M., Akishita, M., Hosoi, T., Toba, K., Kozaki, K., Yoshizumi, M., Ouchi, Y., 2002. Effects of long-term and reduced-dose hormone replacement therapy on endothelial function and intima-media thickness in postmenopausal women. Menopause 9, 58–64.

Hawkins, R.A., Freedman, B., Marshall, A., Killen, E., 1975. Oestradiol-17 beta and prolactin levels in rat peripheral plasma. Br. J. Cancer 32, 179–185.

Hulley, S., Grady, D., Bush, T., Furberg, C., Herrington, D., Riggs, B., Vittinghoff, E., 1998. Randomized trial of estrogen plus progestin for secondary prevention of coronary heart disease in postmenopausal women. Heart and Estrogen/Progestin Replacement Study (HERS) Research Group. JAMA 280, 605–613.

Jick, H., Derby, L.E., Myers, M.W., Vasilakis, C., Newton, K.M., 1996. Risk of hospital admission for idiopathic venous thromboembolism among users of postmenopausal oestrogens. Lancet 348, 981–983.

Joles, J.A., van Goor, H., Koomans, H.A., 1998. Estrogen induces glomerulosclerosis in analbuminemic rats. Kidney Int. 53, 862–868.

Kerdelhue, B., Jolette, J., 2002. The influence of the route of administration of 17beta-estradiol, intravenous (pulsed) versus oral, upon DMBA-induced mammary tumour development in ovariectomised rats. Breast Cancer Res. Treat. 73, 13–22.

Kim, S., Izumi, Y., Izumiya, Y., Zhan, Y., Taniguchi, M., Iwao, H., 2002. Beneficial effects of combined blockade of ACE and AT1 receptor on intimal hyperplasia in balloon-injured rat artery. Arterioscler. Thromb. Vasc. Biol. 22, 1299–1304.

Liu, H.W., Iwai, M., Takeda-Matsubara, Y., Wu, L., Li, J.M., Okumura, M., Cui, T.X., Horiuchi, M., 2002. Effect of estrogen and AT1 receptor blocker on neointima formation. Hypertension 40, 451–457. (discussion 448-450).

Meijs-Roelofs, H.M., Uilenbroek, J.T., De Greef, W.J., De Jong, F.H., Kramer, P., 1975. Gonadotrophin and steroid levels around the time of first ovulation in the rat. J. Endocrinol. 67, 275–282.

Nakaoka, T., Gonda, K., Ogita, T., Otawara-Hamamoto, Y., Okabe, F., Kira, Y., Harii, K., Miyazono, K., Takuwa, Y., Fujita, T., 1997. Inhibition of rat vascular smooth muscle proliferation in vitro and in vivo by bone morphogenetic protein-2. J. Clin. Invest. 100, 2824–2832.

Nozawa, Y., Matsuura, N., Miyake, H., Yamada, S., Kimura, R., 1999. Effects of TH-142177 on angiotensin II-induced proliferation, migration and intracellular signaling in vascular smooth muscle cells and on neointimal thickening after balloon injury. Life Sci. 64, 2061–2070.

Oparil, S., Levine, R.L., Chen, S.J., Durand, J., Chen, Y.F., 1997. Sexually dimorphic response of the balloon-injured rat carotid artery to hormone treatment. Circulation 95, 1301–1307.

Oparil, S., Chen, S.J., Chen, Y.F., Durand, J.N., Allen, L., Thompson, J.A., 1999. Estrogen attenuates the adventitial contribution to neointima formation in injured rat carotid arteries. Cardiovasc. Res. 44, 608–614.

Rossouw, J.E., Anderson, G.L., Prentice, R.L., LaCroix, A.Z., Kooperberg, C., Stefanick, M.L., Jackson, R.D., Beresford, S.A., Howard, B.V., Johnson, K.C., Kotchen, J.M., Ockene, J., 2002. Risks and benefits of estrogen plus progestin in healthy postmenopausal women: principal results From the Women's Health Initiative Randomized Controlled Trial. JAMA 288, 321–333.

Sudoh, N., Toba, K., Akishita, M., Ako, J., Hashimoto, M., Iijima, K., Kim, S., Liang, Y.Q., Ohike, Y., Watanabe, T., Yamazaki, I., Yoshizumi, M., Eto, M., Ouchi, Y., 2001. Estrogen prevents oxidative stress-induced endothelial cell apoptosis in rats. Circulation 6;103 (5), 724–729.

Tazawa, S., Nakane, T., Chiba, S., 1999. Angiotensin II type 1 receptor blockade prevents up-regulation of angiotensin II type 1A receptors in rat injured artery. J. Pharmacol. Exp. Ther. 288, 898–904.

Tolbert, T., Thompson, A., Bouchard, P., Oparil, S., 2001. Estrogen-induced vasoprotection is independent of inducible nitric oxide synthase expression. Evidence from the mouse carotid artery ligation model. Circulation 104, 2740–2745.

Tomiyoshi, Y., Sakemi, T., Aoki, S., Miyazono, M., 2002. Different effects of castration and estrogen administration on glomerular injury in spontaneously hyperglycemic Otsuka Long-Evans Tokushima Fatty (OLETF) rats. Nephron 92, 860–867.

Wakatsuki, A., Okatani, Y., Ikenoue, N., Shinohara, K., Watanabe, K., Fukaya, T., 2003. Effect of lower dose of oral conjugated equine estrogen on size and oxidative susceptibility of low-density lipoprotein particles in postmenopausal women. Circulation 108, 808–813.

Wakatsuki, A., Ikenoue, N., Shinohara, K., Watanabe, K., Fukaya, T., 2004. Effect of lower dosage of oral conjugated equine estrogen on inflammatory markers and endothelial function in healthy postmenopausal women. Arterioscler. Thromb. Vasc. Biol. 24 (3), 571–576.

White, C.R., Shelton, J., Chen, S.J., Darley-Usmar, V., Allen, L., Nabors, C., Sanders, P.W., Chen, Y.F., Oparil, S., 1997. Estrogen restores endothelial cell function in an experimental model of vascular injury. Circulation 96, 1624–1630.

Xu, Y., Arenas, I.A., Armstrong, S.J., Davidge, S.T., 2003. Estrogen modulation of left ventricular remodeling in the aged heart. Cardiovasc. Res. 57, 388–394.

Available online at www.sciencedirect.com

SCIENCE DIRECT

Life Sciences 75 (2004) 1219–1229

Life Sciences

www.elsevier.com/locate/lifescie

Caveolin-1, Id3a and two LIM protein genes are upregulated by estrogen in vascular smooth muscle cells

Tokumitsu Watanabe[a], Masahiro Akishita[b], Takashi Nakaoka[c], Hong He[a], Yukiko Miyahara[a], Naohide Yamashita[c], Youichiro Wada[d], Hiroyuki Aburatani[d], Masao Yoshizumi[e], Koichi Kozaki[a], Yasuyoshi Ouchi[a,*]

[a] *Department of Geriatric Medicine, Graduate School of Medicine, University of Tokyo 7-3-1 Hongo, Bunkyo, Tokyo 113-8655, Japan*

[b] *Department of Geriatric Medicine, Kyorin University School of Medicine, Tokyo 181-8611, Japan*

[c] *Department of Advanced Medicine, Institute of Medical Science, University of Tokyo, Tokyo 108-8639, Japan*

[d] *Genomic Science Division, Research Center for Advanced Science and Technology, University of Tokyo, Tokyo, Japan*

[e] *Department of Cardiovascular Physiology and Medicine, Graduate School of Biomedical Sciences, Hiroshima University, Hiroshima, Japan*

Received 3 September 2003; accepted 2 March 2004

Abstract

Estrogen has diverse effects on the vasculature, such as vasodilation, endothelial growth and inhibition of vascular smooth muscle cell (VSMC) proliferation and migration. However, little is known about the genes that are regulated by estrogen in the vascular wall. Wistar rats were ovariectomized or sham-operated (Sham group), and 2 weeks after the operation, were subjected to subcutaneous implantation of placebo pellets (OVX + V group) or estradiol pellets (OVX + E group). Endothelium-denuded aortic tissue was examined 2 weeks after implantation. By applying high-density oligonucleotide microarray analysis, the expression of approximately 7000 genes was analyzed. Among the genes with different expression levels between the OVX + E group and the OVX + V group, those that have been reported to be expressed in the vasculature or muscle tissue, were chosen. Finally, four genes, caveolin-1, two LIM proteins (enigma and SmLIM) and Id3a, were identified. Microarray as well as real-time polymerase chain reaction showed that the expression levels of these genes were significantly higher in the OVX + E group than in the OVX + V group. To clarify whether estrogen directly upregulates these genes in the vascular wall, Northern blot analysis was performed using cultured rat VSMC. Addition of 100 nmol/L estradiol for 24 hours increased the mRNA levels of all four genes. Although the

* Corresponding author. Tel.: +81-3-5800-8830; fax: +81-3-5800-6530.
E-mail address: youchi-tky@umin.ac.jp (Y. Ouchi).

0024-3205/$ - see front matter
doi:10.1016/j.lfs.2004.03.004

precise mechanism remains unclear, regulation of these genes by estrogen might contribute to its effect on VSMC.

Keywords: Atherosclerosis; Gene expression; Hormones; Smooth muscle

Introduction

Epidemiological studies have shown that the risk for cardiovascular disease is lower in premenopausal women than in men of the same age. Hormone replacement therapy has been reported to lower the incidence of cardiovascular disease in postmenopausal women (Colditz et al., 1987; Kannel et al., 1976), although the beneficial effects of estrogen have not been confirmed in recent randomized trials (Hulley et al., 1998; Rossouw et al., 2002). A number of animal studies have also shown estrogen's anti-atherogenic effects, including amelioration of the response to vascular injury (Sullivan et al., 1995), inhibition of endothelial cell apoptosis (Sudoh et al., 2001), and nitric oxide-mediated vasodilatation (Bell et al., 1995). Estrogen receptors (ER) are expressed in the vasculature (Hodges et al., 2000; Karas et al., 1994), supporting that estrogen can exert its effect directly on the vascular wall.

Several estrogen-responsive genes, such as pS2 (Brown et al., 1984), c-fos (Weisz and Bresciani, 1988), and efp (Inoue et al., 1993), have already been identified in reproductive tissues. In the vasculature, estrogen-regulated genes without estrogen-responsive elements in their promoter region are reported (Akishita et al., 1996; Gallagher et al., 1999; Nickenig et al., 1998). The expression of c-fos (Akishita et al., 1996), angiotensin-converting enzyme (Gallagher et al., 1999), and angiotensin receptor-1 (Nickenig et al., 1998) in the aorta was downregulated by estrogen replacement in ovarietomized rats. These changes of gene expression could explain a part of atheroprotective effects of estrogen. Recently, methods for global gene analysis have been developed, and among them, the high-density oligonucleotide microarray, has come to be used as a powerful tool by many investigators. In this study, to discover new genes that might play a role in the action of estrogen, we performed microarray analysis to identify genes that are differentially expressed in the vascular wall, especially in vascular smooth muscle cells (VSMC), before and after treatment with estrogen. To confirm the results obtained from the microarray, we performed real-time polymerase chain reaction (PCR) and Northern blotting. Finally, four genes were identified as novel estrogen-regulated genes in VSMC.

Methods

Animals

Eight-week-old female Wistar rats (Oriental Yeast, Co., Ltd., Tokyo, Japan) were used in this study. They were kept individually in stainless-steel cages in a room where lighting was controlled (12 hours on, 12 hours off) and room temperature was kept at around 22 °C. They were given a standard diet and water ad libitum. All the surgical procedures were performed under ether anesthesia. All of the experimental protocols were approved by the Animal Research Committee of the University of Tokyo.

Ovariectomy and E2 Implantation

Rats were randomly divided into three groups. Two groups of rats were ovariectomized and the other group of rats was sham-operated. After a two-week recovery period, one group of ovariectomized rats (OVX + E group, n = 5) underwent subcutaneous implantation of a three-week releasing pellet containing 0.5 mg 17β-estradiol (E2; Innovative Research of America). The other group of ovariectomized rats (OVX + V group, n = 5) and sham-operated rats (Sham group, n = 4) received placebo pellets. Two weeks after pellet implantation, blood samples were obtained from rats. Serum estradiol concentration was 5.6 ± 1.5 pg/ml in the Sham group (n = 4), 2.8 ± 1.0 pg/ml in the OVX + V group (n = 5), and 74.5 ± 12.1 pg/ml in the OVX + E group (n = 5). The thoracic aorta was obtained from rats after sacrifice. The endothelium was removed from the aorta by scraping with blade to ensure that the sample was mainly derived from VSMC.

High-density oligonucleotide microarray analysis

Total RNA was extracted from the aorta with Isogen (Wako Junyaku Ltd.) according to the manufacturer's instructions. One microgram of RNA isolated from the aorta of OVX + E group, OVX + V group and Sham group (n = 2, each group) rats was amplified up to approximately 100 μg cRNA and hybridized to the high-density oligonucleotide microarray (GeneChip Rat GenomeU34A; Affymetrix, Santa Clara, CA) as described previously (Ishii et al., 2000). This array contains probes interrogating approximately 7000 full-length rat genes. The intensity for each feature of the array was calculated by using Affymetrix Gene Chip version 3.3 software. The average intensity was made equal to the target intensity, which was set at 100, to reliably compare variable multiple arrays. In addition to the default parameters of the software, we added a criteria that >100 average intensity units per transcript was required for a gene to be considered "present" in the samples. Genes, with an intensity of around 1.5-fold higher or lower in the OVX + E group than in the OVX + V group, were identified.

Real-time PCR

Total RNA was treated with DNase (Progema) at 37°C for 1 h. One microgram of RNA was reverse transcribed into cDNA using Oligo dT primer (GIBCO) and an Ominiscript kit (GIBCO). Real-time PCR was carried out in an iCycler (BioRad) at 95°C for 15 min to activate HotStar Taq DNA polymerase, followed by 35 cycles of 94°C for 15 sec, 55°C for 30 sec and 72°C for 30 sec using a SYBR green assay kit (TAKARA). Amplicons were around 100 bp long. We selected the primer sets that amplified the sequences as close as possible to the 3′ coding region of the target genes. The sequences of the primers are shown in Table 1. The expression levels of each gene were normalized for glyceraldehyde-3-phosphate dehydrogenase expression.

Cell culture

VSMC were harvested from the aorta of Wistar rats by enzymatic dissociation, as previously reported (Watanabe et al., 2001). Cells were maintained in Dulbecco's modified Eagle's medium (Nikken Bio Medical Laboratory, Tokyo) supplemented with 10% fetal bovine serum (Intergen Co., Purchase, NY), penicillin (100 U/ml) and streptomycin (100 μg/ml) at 37°C in a humidified atmosphere of 95% air and

Table 1
Primers used for quantification of mRNA levels

Accession no.	Definition	Forward primer	Reverse primer
U48247	Enigma	ttcgtctccaccaaacactg	tccctctgctagctcctgag
Z46614	Caveolin1	gcatcctctctttcctgcac	tggaatagacacggctgatg
U44948	SmLIM	taatgtggatggccttaccg	ggatgggcaggagagtgtag
AF000942	Id3a	cctcgaccttcaagtggttc	acgttcagatgagcctggtc
M17701	Glyceraldehyde-3-phosphate-dehydrogenase	cttccgtgttcctaccc	acctggtcctcagtgtagcc
M83107	SM22	tgagcaagttggtgaacagc	attgagccacctgttccatc
X06801	αSMactin	gctctggtgtgtgacaatgg	aaccatcactccctggtgtc
U50044	von Willebrand factor	agcgggtgaaatacctagcc	gcagtcagttggcctctacc

5% CO2. VSMC at 6–10 passages were used in the experiments. Cells were seeded in 10-cm-culture dishes to grow to confluence. Then, the medium was replaced with phenol red-free RPMI1640 (Sigma) containing 100 nM E2 (Sigma) or vehicle (0.1% ethanol). Twenty-four hours later, cells were washed with phosphate-buffered saline twice and homogenized immediately in Isogen reagent (Nippon Gene, Osaka, Japan).

Northern blot analysis

Twenty micrograms of total RNA from cultured VSMC were fractionated on 1.3% formaldehyde-agarose gel and transferred to nylon filters (Hybond-N, Amersham Life Science Inc.). The filters were hybridized with random-primed ^{32}P-labeled rat cDNA probes and autoradiographed. To synthesize cDNA probes, reverse transcription-PCR was performed using RNA prepared from VSMC with primers specific for each gene. The primers were synthesized according to the published rat cDNA sequences as follows: (forward/reverse)

Enigma: 5′-gccttctcagcagtcagctt-3′/5′-ttcttctggatgccaggact-3′
Caveolin-1: 5′-cgtagactccgagggacatc-3′/5′-gctcttgatgcacggtacaa-3′
Smooth muscle LIM protein (SmLIM): 5′-gaagaggtgcagtgtgatgg-3′/5′-tctggagcacttctcagcac-3′
Inhibitor of DNA binding 3a (Id3a): 5′-ggaacgtagcctagccattg-3′/5′-ttcagatgagcctggtctagc-3′.

Amplified PCR products were subcloned into a plasmid vector, pCR2.1 vector, and sequenced. An oligonucleotide probe complementary to 18S rRNA was used to confirm the equal loading of RNA. (Watanabe et al., 2001) The filters were autoradiographed, and the bands were scanned and the density was determined with Scion software (Scion image ver 3.0, Scion Corp.).

Statistical analysis

The mRNA levels calculated in real-time PCR were analyzed using one-way ANOVA. When a statistically significant effect was found, Newman-Keul's test was performed to isolate the difference between the groups. A value of $P < 0.05$ was considered significant. All data in the text and figures are expressed as mean ± SE.

Results

Screening for genes expressed differently between OVX + V and OVX + E by high-density oligonucleotide array

We first performed a global expression analysis of approximately 7000 genes using a high-density oligonucleotide microarray to identify estrogen-regulated genes in the rat aorta. Around 2000 genes were considered to be present in the aorta according to our criteria. As shown in Table 2, the expression of control GAPDH was comparable among the groups, suggesting that the microarray assay worked well. The expression of SM22 was high, whereas that of von Willebrand factor and endothelial nitric oxide synthase was below the detection level. These findings indicate that the samples were mainly derived from the medial layer of the aorta. In this screening, we identified approximately 200 genes, the expression levels of which were different between the OVX + E group and OVX + V group. We, first, checked the genes reported to be regulated by estrogen in the aorta, such as angiotensin II type 1 receptor (Nickenig et al., 1998), angiotensin converting enzyme (Gallagher et al., 1999), and c-fos (Akishita et al., 1996), and in reproductive tissues, such as progesterone receptor (May et al., 1989), c-myc (Weisz and Bresciani, 1988), and glucose-6-phosphate dehydrogenase (Korach et al., 1985). Consistent with the previous data, the intensity of angiotensin converting enzyme in OVX + E was down-regulated to nearly 50% compared to that in OVX + V. However, AT1 receptor, c-myc and progesterone receptor were not detected in aorta by high-density oligonucleotide microarray analysis probably because of the low sensitivity to these genes. Also, in sham-operated rats, the intensity of c-fos gene was at much higher level compared to that in OVX + V. The reason for a tremendous increase of c-fos expression might result from unknown stresses, because the intensity of several immediate-early genes was also increased in sham-operated rats (data not shown). The explanations for these results were that the sensitivity of probes for several genes was under the threshold, and/or that the reproducibility was not high due to small number of samples in each group (n = 2). Then, among the 200 genes, we focused on up to 20 candidate genes, which were reported to be expressed in the vasculature.

Table 2
Expression of marker genes and previously reported estrogen-regulated genes in aorta

Accession No.	Definition	Sham (Intensity)	OVX+V (Intensity)	OVX+E (Intensity)
M17701	Glyceraldehyde-3-phosphate-dehydrogenase	1278.5	1232.6	1246.0
M83107	SM22	4350.8	4487.8	4631.9
U50044	von Willebrand factor	8.7	-54.8	-19.8
AF110508	endothelial nitric oxide synthase	48.4	48.1	45.3
M90065	angiotensin II receptor	-7.5	5.1	4.2
U03734	angiotensin converting enzyme	216.6	239.9	148.3
X06769	c-fos	1800.1	307.7	231.8
S64044	progesterone receptor	61.3	31.7	39.8
X07467	glucose-6-phosphate dehydrogenase	474.0	332.1	454.2
Y00396	c-myc	44.4	36.3	33.3

Table 3
Genes with altered expression level in aorta according to DNA microarray technique

Accession no.	Definition	Sham (intensity)	OVX+V (intensity)	OVX+E (intensity)	OVX+E/OVX+V
U48247	Enigma	288.3	128.6	455.5	3.5
Z46614	Caveolin-1	674.3	329.1	694.4	2.1
U44948	SmLIM	1266.9	1260.7	2054.9	1.6
AF000942	Id3a	201.7	224.6	318.3	1.4

Confirmation of estrogen-regulated genes in aorta by real-time PCR

Next, we performed real-time PCR to examine the expression of the candidate genes obtained from the microarray. In real-time PCR, we used primers that amplified sequences different from the microarray. Subsequently, four genes, caveolin1, enigma, SmLIM and Id3a, were identified as being upregulated in the OVX + E group (Table 3 and Fig. 1). On the other hand, we could not identify any genes down-regulated in the OVX + E group in this study, so far. To exclude the possibility of the contamination with other cell types in total RNA samples we used, we compared the intensity of these four genes and markers for endothelium or VSMC in the samples between with or without endothelium obtained from intact 8-week-old male rats (n = 12) (Fig. 2). Semi-quantitative analysis by real-time PCR showed that these four genes and markers of VSMC were expressed comparably between samples with or without endothelium. In contrast, the expression of an endothelial marker, von Willebrand factor, was scanty in endothelium-denuded samples. Specific markers for adventitial fibroblasts have not been identified (Sartore et al., 2001). Therefore, we cannot exclude the contamination with adventitial fibroblasts, although the adventitial layer is very small in amount compared with smooth muscle layers.

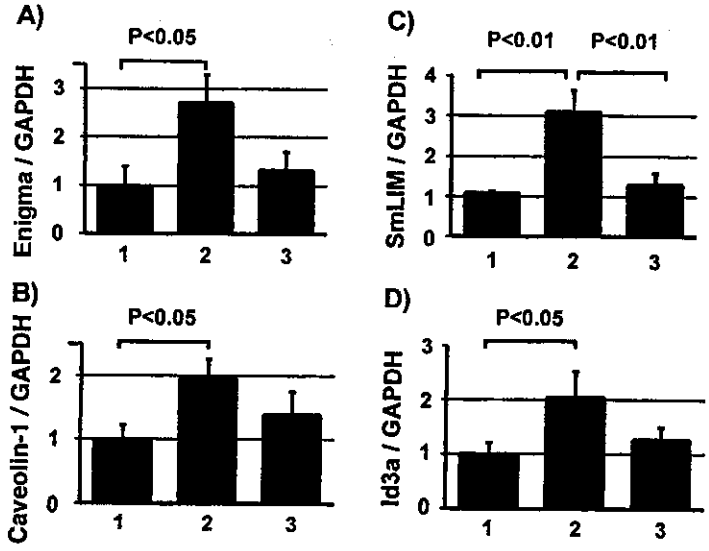

Fig. 1. Real-time PCR comparing expression of enigma, caveolin-1, SmLIM and Id3a in aortic tissue. Total RNA was obtained from the aorta of OVX + V (lane 1, n = 5), OVX + E (lane 2, n = 5), and Sham (lane 3, n = 4) groups, and reverse-transcribed into cDNA. Then, 50 ng cDNA was amplified using primers specific for each gene sequence using real-time PCR method. The starting quantities were calculated and expressed as the ratio of each gene to GAPDH. Values are shown as mean ± SE.

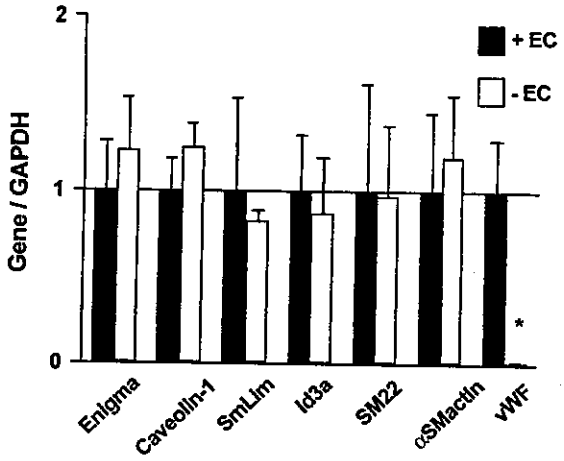

Fig. 2. The expression levels in the identified genes and maker genes in the samples with or without endothelium (EC). The aortic tissues were obtained from intact 8-week male rats, and were divided into two groups; with EC (n = 6) and without EC (n = 6). Real-time PCR was performed as described above, and the starting quantities were calculated and expressed as the ratio of each gene to GAPDH. Values are shown as the ratio of the samples with EC to that without EC and as mean ± SE. *, $p < 0.01$ vs + EC. EC; endothelium, vWF; von Willebrand factor.

E2-induced expression of genes in cultured VSMC

In order to investigate whether E2 could directly regulate the expression of these four genes, we examined their mRNA levels in cultured VSMC by Northern blot analysis. As shown in Fig. 3, treatment with E2 for 24 hours increased the mRNA levels of caveolin1, enigma, SmLIM and Id3a mRNA.

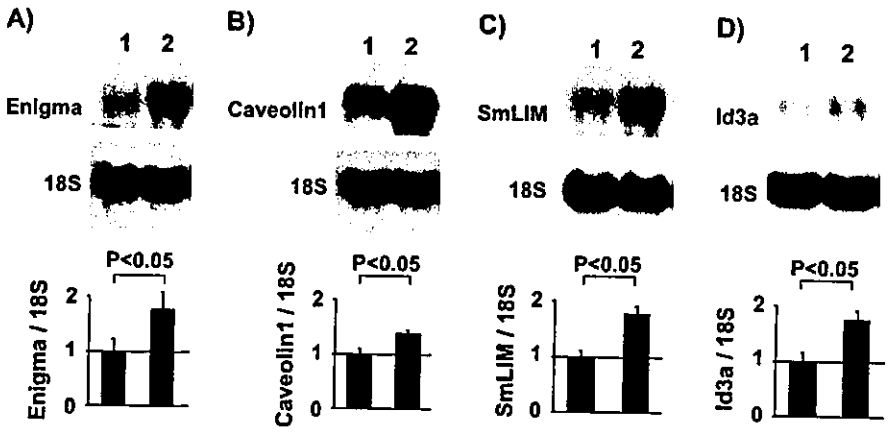

Fig. 3. Northern blot analysis of enigma, caveolin-1, SmLIM1 and Id3a in cultured VSMC. VSMC were treated with vehicle (lane 1) or 100 nmol/L E2 (lane 2) for 24 hours. Total RNA was extracted from VSMC, and 20 μg total RNA per lane was used for Northern blot analysis. The membrane was hybridized to a 32P-labeled cDNA probe specific for each gene and to an 18S probe to assess loading differences. In different sets of experiments, mRNA levels of indicated genes were measured by densitometry and expressed as the ratio of genes to 18S. Similar results were obtained in three independent experiments.

Discussion

In the present study, we screened for genes that responded to estrogen stimulation in VSMC. We newly identified genes upregulated by estrogen; enigma, SmLIM, caveolin and Id3a, in VSMC.

Caveolin-1 is one subtype of caveolins, which are principal coat proteins of caveolae (Severs, 1988). Caveolae, the flask-shaped vesicular invaginations of the plasma membrane, are present in many cell types including VSMC (Drab et al., 2001). Caveolae function in signal transduction (Okamoto et al., 1998) as well as in endocytosis and transcytosis in vesicular transport (Schnitzer et al., 1995). Mice lacking the caveolin-1 gene show impaired endothelium-dependent relaxation, contractility and maintenance of myogenic tone of the aorta through nitric oxide and Ca^{2+} signaling (Drab et al., 2001). Several studies have reported the role of caveolin-1 in estrogen-mediated signaling in vascular cells. In vascular endothelium, nitric oxide synthase is activated rapidly by estrogen following binding with ERα in caveolae (Chambliss et al., 2000). In VSMC, estrogen stimulated the binding of ERα with caveolin-1 and augmented the production of caveolin-1 through a transcriptional mechanism (Razandi et al., 2002). Consistent with this report, we showed that estrogen upregulated mRNA expression of caveolin-1 in the aorta, as well as in cultured VSMC. Taken together, estrogen-mediated upregulation of cavelin-1 might be related to the improvement of vascular function.

Two LIM protein genes and one member of the Id gene family were also identified as estrogen-regulated genes in the aorta in the present study. LIM proteins are a protein family containing the LIM motif, a double-zinc-finger structure. The LIM motif has been proposed to participate in protein-protein interactions (Dawid et al., 1995; Sanchez-Garcia and Rabbitts, 1994), and to be critical in cellular determination and differentiation (Arber and Caroni, 1996; Schmeichel and Beckerle, 1994). SmLIM, one of the LIM proteins, is expressed principally in VSMC of adult animals and is induced in VSMC during development, preceding the appearance of the smooth muscle myosin heavy chain, a sensitive indicator of VSMC differentiation (Jain et al., 1998). Moreover, SmLIM localizes in the nucleus and in actin-based filaments in the cytosol. Therefore, SmLIM is thought to coordinate cytoskeletal function and subsequently regulate cellular proliferation and differentiation (Jain et al., 1998). Another LIM protein, enigma, belongs to the PDZ-LIM protein, and is expressed abundantly in skeletal muscle as well as in non-muscle cells (Durick et al., 1998; Guy et al., 1999). The PDZ domain of enigma binds to a skeletal muscle target, the actin-binding protein, tropomyosin, suggesting that enigma is an adapter protein that directs the LIM-binding protein to actin filaments of muscle cells (Guy et al., 1999). The inhibitor of DNA binding (Id), a class of helix-loop-helix transcription factors, is known to regulate growth in many cells including VSMC (Matsumura et al., 2001; Norton et al., 1998; Olson, 1990). There are four known Id genes, Id1 to Id4. Id3a is produced by alternative splicing of the Id3 gene, resulting in inclusion of a 115-bp "coding intron", which encodes a unique 29-amino-acid carboxyl terminus of the Id3a protein (Matsumura et al., 2001). It is reported that Id3a is associated with apoptotic activity in VSMC (Matsumura et al., 2001). In contrast, another group showed that Id3 mediated angiotensin II-induced cell growth (Mueller et al., 2002); therefore, the precise role of Id3 and its splice variant, Id3a, in the vasculature, has not been determined.

There are no reports with respect to the regulation of these three genes by estrogen, not only in the vasculature but also in other organs, so our findings might imply a new understanding of mechanisms of the effects of estrogen in the vascular wall. Because SmLIM and Id3a may be associated with cell growth and differentiation, these genes might mediate the effects of estrogen on VSMC growth and differentiation. Enigma is considered to be an adaptor protein, which can connect some kinases or